A SPLIT CONFIGURATION HYBRID ELECTRIC VEHICLE MODEL FOR THE NADS

Chris Schwarz
National Advanced Driving Simulator
The University of Iowa
2401 Oakdale Blvd
Iowa City, IA 52242
319-335-4642
319-335-4658 (fax)
cschwarz@nads-sc.uiowa.edu

Submitted July 22, 2001

ABSTRACT

In order to remain on the forefront of driving simulation technology, it is necessary to continually upgrade and expand the capabilities of the NADS. One extension that is suggested by recent trends in the automotive marketplace is the ability to simulate hybrid electric vehicles. Support of hybrid electric vehicles by the NADS is motivated by the engineering and human factors challenges of designing and testing advanced concepts for vehicles and user interfaces. This paper discusses the extension of the vehicle dynamics to include a split hybrid electric four wheel drive power train. The new power train is based on Daimler Chrysler's Dodge Durango TTR hybrid. The vehicle dynamics subsystem is based on the University of Iowa's real time recursive dynamics (RTRD). The RTRD enables efficient simulation of general rigid multi-body systems. Additional force generating subroutines are included to model an extensive array of vehicle subsystems, such as power train, steering, brakes, aerodynamics, and tires. The new hybrid power train design includes new electromechanical component models, which are described in detail. A discussion of appropriate applications of the models based on their fidelity is included. Models of electromechanical components can bring with them greater bandwidth requirements. Bandwidth/performance tradeoffs are discussed; and suitable models for driver-in-the-loop simulation are selected.

INTRODUCTION

The National Advanced Driving Simulator (NADS) will expand the capabilities for human centered driving simulator research in the improvement of vehicle safety and usability as well as the improvement of their efficiency and performance. The large excursion motion base allows the driver to have greater sensitivity to the motion cues of the vehicle. This represents an opportunity for more detailed vehicle design studies as well as a responsibility for accurate, high fidelity vehicle models. The NADS is equipped with four validated vehicle models along with their corresponding cabs. In order to remain on the forefront of driving simulation research, however; it is necessary to continually upgrade its technology and capabilities. It is envisioned that as new vehicle models are added to the NADS library, new cabs will also be acquired and instrumented for use in the simulator. Possible a generic cab with highly configurable dashboard panels would be used for increased flexibility and modularity.

One extension suggested by recent trends in the automotive marketplace is the ability to model hybrid electric vehicles. The Toyota Prius and Honda Insight are popular hybrids currently available in the US; and new models are due out from Ford, GM, and Daimler Chrysler in the next couple of years. Support of hybrid electric vehicles by the NADS is motivated by the engineering and human factors challenges of designing and testing advanced concepts for vehicles and user interfaces. This paper discusses the extension of the vehicle dynamics to include a split hybrid electric four wheel drive powertrian. This configuration is based on the Daimler Chrysler Dodge Durango hybrid forecasted for production in 2003 [1]. The hybrid version of the Durango would offer V8 performance with a V6 engine while improving gas mileage by 20%. This split configuration hybrid is called through-the-road (TTR) because the only connection between the electric and gas powered systems is between the tire forces, through the road.

The vehicle dynamics core used in the NADS is based on the University of Iowa's real time recursive dynamics (RTRD) code. The RTRD is an efficient method of simulating rigid multibody dynamic systems. It supports several types of joints and force generating elements appropriate for use in vehicle modeling. This core, along with vehicle subsystems for tire, brakes, steering, aerodynamics, and powertrain were enhanced by NHTSA and VRTC for integration into the NADS [2,3,4]. VRTC also designed and validated vehicle models for the Ford Taurus, Jeep Cherokee, Chevy Malibu, and Freightliner class 8 truck. The Jeep Cherokee is used as the base vehicle for the split hybrid described in this paper. Details on the Cherokee model are available in the literature [5,6].

The NADS simulation center has been involved in developing a hybrid electric simulation capability through DARPA programs targeted on advanced propulsion vehicles. A series hybrid powertrain baseline was first developed and then expanded to support one, two, and four motor configurations. Vehicle models employing these powertrains have been driven on a PC based simulator and at the Iowa Driving Simulator (IDS), but not yet tested on the NADS. In the sequel, the split configuration hybrid will be described and each component model created to support this configuration presented. Discussion of appropriate applications of the models based on their fidelity is included. A bandwidth/performance tradeoff in the motor model fidelity is also investigated.

SPLIT HYBRID MODEL

The base vehicle model targeted for conversion is the Jeep Cherokee model developed by VRTC [5,6]. The Cherokee has two and four wheel drive modes. It has a solid rear axle with leaf spring suspension. Complete data on the sizing of the engine, brakes, and powertrain is reported in the VRTC papers. In this paper we describe how the vehicle powertrain has been hybridized. The sizing of the motor, engine, battery, and gear ratios is a process that trades off several vehicle performance specification, including total power and torque capability, front/rear power and torque splits, base vehicle speed for full motor torque capacity, weight and space requirements, etc. The purpose of this paper is not to explore these design tradeoffs. Rather, a real-time simulation capability is presented for use in the NADS by industry, university, and government clients interested in advanced propulsion vehicles. Most likely, the client will have a set of vehicle specifications or model parameters, which will be used to modify the nominal model presented here.
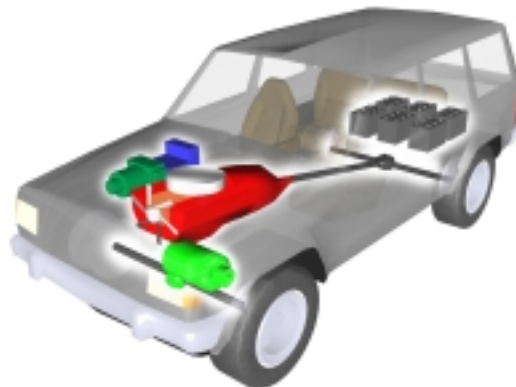

Figure 1. Hybrid Electric Jeep Cherokee Concept

Following the design of the TTR Durango, the Jeep engine torque map is de-rated by 30%, effectively reducing it from a V8 to a V6 engine. The transfer case is removed completely. Instead, an induction motor powered through an inverter by a battery pack is connected to the front differential. The transmission is not modified at all and serves to define the gear ratio between the engine and the rear wheels. The total gear ratio from the motor to the front wheels is constant and should be sized according to the desired vehicle specifications for front/rear torque split and efficient motor operation. Apart from the hardware modifications, an Energy Management System (EMS) provides the necessary control over the motor based on what it senses the vehicle is presently doing. A conceptual picture of the hybrid electric Jeep Cherokee is shown in figure 1.

2

Hybrid Electric Component Modeling

Induction Motor

A three phase induction motor is used as the electromechanical prime mover. Induction motors have long been used in numerous applications ranging from fractional horsepower to several hundred horsepower in size. A typical squirrel cage induction motor has three identical windings on the stator. The rotor may consist of a series of conducting bars embedded in a ferromagnetic material. The currents induced in the rotor magnetize it, allowing the generation of electromotive force, or torque. Rotor currents are generated when there is slip between the frequency of the stator voltage supply and the equivalent electrical frequency of the rotor, given by its rotational frequency multiplied by the number of pole pairs in the rotor.

Analysis and simulation of the induction machine is simplified by transforming the voltage equations into a rotating reference frame via the so-called Parks transformation. For balanced operation, a reference frame that rotates synchronously with the electrical supply frequency is particularly useful, as it results in DC voltages and currents at steady state. The resulting reference frame is referred to as the dq0 frame, while the original three phase reference frame shall be denoted as the abc frame.

Full Order Model The theory and analysis of induction machines is presented in [7]. Several useful discussions on computer implementations of electromechanical machines are found therein. One such discussion recommends the computer implementation of a rotating machine to use the rotor and stator flux linkages as states rather than the rotor and stator currents. This choice reduces the number of derivative terms in the formulation and results in slightly lower frequency content in the states. The further assumption of balanced operation is made which allows the elimination of the 0s and 0r states from the dq0 frame of reference. The voltage equations for the balanced three-phase induction motor in the synchronously rotating reference frame are given by

$$
\begin{bmatrix} \dot{\psi}_{qs} \\ \dot{\psi}_{ds} \\ \dot{\psi}_{qr} \\ \dot{\psi}_{dr} \end{bmatrix} = \begin{bmatrix} -\dfrac{r_s L_{rr}}{D} & -\omega_e & \dfrac{r_s M}{D} & 0 \\[2ex] \omega_e & -\dfrac{r_s L_{rr}}{D} & 0 & \dfrac{r_s M}{D} \\[2ex] \dfrac{r_r M}{D} & 0 & -\dfrac{r_r L_{ss}}{D} & -(\omega_e - \omega_s) \\[2ex] 0 & \dfrac{r_r M}{D} & (\omega_e - \omega_s) & -\dfrac{r_r L_{ss}}{D} \end{bmatrix} \begin{bmatrix} \psi_{qs} \\ \psi_{ds} \\ \psi_{qr} \\ \psi_{dr} \end{bmatrix} + \begin{bmatrix} v_{qs} \\ v_{ds} \\ v_{qr} \\ v_{dr} \end{bmatrix} \qquad (1)
$$

Where the denominator term is defined by

$$ D = L_{ss} L_{rr} - M^2 $$

L_{rr}, L_{ss}, and M denote the rotor, stator, and mutual inductance in the motor respectively. The rotor and stator resistances are denoted by r_r and r_s. ω_e is the frequency of the stator voltage supply, while ω_s is the equivalent electrical frequency, which is given by

$$ \omega_s = \frac{P}{2} \omega_r $$

Where P is the number of electrical poles in the rotor and ω_r is the mechanical angular rotor speed. The states are flux linkages and the inputs are voltages. Normally, the rotor voltages are not applied and are set to zero. The resulting motor torque can be written as a function of flux linkages as

3

$$\tau_e = \frac{3}{2}\frac{P}{2}\frac{M}{D}\left(\psi_{qs}\psi_{dr} - \psi_{ds}\psi_{qr}\right) \tag{2}$$

If an efficiency map is available for the motor, it may be used to modify the torque in both motoring and generating modes of operation.

Reduced Order Model It was discussed in [7] that a reduced order model of the induction machine is often used in the analysis of large scale power systems. The reduced order model neglects the transients in the stator variables but is nevertheless suitable for analyzing large excursions in the motor's region of operation, which is something a linearized model is not capable of. The reduced order model is applicable as long as the following assumptions are met

1. Transients in the power supply are not analyzed

2. The three phase supply voltage is balanced

If one neglects the stator derivatives in (1), a DAE of index one is obtained. This DAE can be directly reduced to an ODE through substitution. The new state equations for the rotor flux linkages are given in matrix form by

$$\begin{bmatrix} \dot{\psi}_{qr} \\ \dot{\psi}_{dr} \end{bmatrix} = \begin{bmatrix} \dfrac{r_r M}{D} & 0 & -\dfrac{r_r L_{ss}}{D} & -\left(\omega_e - \omega_s\right) \\ 0 & \dfrac{r_r M}{D} & \left(\omega_e - \omega_s\right) & -\dfrac{r_r L_{ss}}{D} \end{bmatrix} \begin{bmatrix} \psi_{qs} \\ \psi_{ds} \\ \psi_{qr} \\ \psi_{dr} \end{bmatrix} + \begin{bmatrix} v_{qs} \\ v_{ds} \\ v_{qr} \\ v_{dr} \end{bmatrix} \tag{3}$$

where the stator flux is now calculated as

$$\begin{bmatrix} \psi_{qs} \\ \psi_{ds} \end{bmatrix} = \frac{1}{WD}\begin{bmatrix} \dfrac{r_s^2 L_{rr} M}{D} & -\omega_e r_s M \\ \omega_e r_s M & \dfrac{r_s^2 L_{rr} M}{D} \end{bmatrix} \begin{bmatrix} \psi_{qr} \\ \psi_{dr} \end{bmatrix} + \frac{1}{W}\begin{bmatrix} -\dfrac{r_s L_{rr}}{D} & \omega_e \\ -\omega_e & -\dfrac{r_s L_{rr}}{D} \end{bmatrix} \begin{bmatrix} v_{qs} \\ v_{ds} \end{bmatrix} \tag{4}$$

with

$$W = \omega_e^2 + \frac{r_s^2 L_{rr}^2}{D^2}$$

These equations are suitable for computer implementation employing a standard ODE integrator.

Motor Controller

Many strategies exist at this time to control induction motors ranging from simple, constant volts-hertz ratio strategies to intelligent, nonlinear controllers. The controller selected in the real-time environment should be easy to implement and of similar fidelity as the motor model. Vector control meets these requirements and provides accurate control of the motor at all speeds. Vector control methods try to decouple the d and q axes of the model so that it is effectively controlled like a DC motor. Control of DC machines is simpler and well understood. An overview of vector control is found in [8]. In keeping with the decision to choose flux linkages as states, the vector control formulation is derived in terms of flux rather than current as it is presented in [8].

Vector controllers maintain decoupling by forcing the q axis rotor flux linkage to zero. All the rotor flux is contained in the d component and a constant value is commanded except at high speeds, when flux deterioration begins. Desired rotor flux is written as

$$\psi_r^* = f\left(\omega_s\right)$$

It is obvious from (2) that the only torque producing component of the stator flux is from the q axis if ψ_{qr} is zero. The desired value for this flux is easily computed from the desired torque as

$$\psi_{qs}^* = \frac{\tau_e^*}{\dfrac{3}{2}\dfrac{P}{2}\dfrac{M}{D}\psi_r^*}$$

Decoupling is maintained by controlling the slip frequency appropriately as a function of the rotor and stator desired flux. It is found from the steady state solution of (1) with the q axis rotor flux set to zero as

$$\omega_{sl}^* = \frac{r_r M}{D}\frac{\psi_{qs}^*}{\psi_r^*}$$

The commanded stator frequency is calculated as the equivalent electrical frequency of the rotor plus the commanded slip frequency.

$$\omega_e = \omega_{sl}^* + \omega_s$$

The control voltages may then be directly calculated from the desired flux as

$$\begin{bmatrix} v_{qs}^* \\ v_{ds}^* \end{bmatrix} = \begin{bmatrix} -\dfrac{r_s L_{rr}}{D} & -\omega_e \dfrac{L_{ss}}{M} \\ \omega_e & -\dfrac{r_s}{M} \end{bmatrix} \begin{bmatrix} \psi_{qs}^* \\ \psi_r^* \end{bmatrix}$$

Battery

The battery model used is similar to the one presented in [9]. It is assumed that the voltage of the battery can be calculated from the simple electrical relation

$$v = V_b + r_b I_b \in \left[0, V_b\right]$$

The internal resistance is modeled as a curve dependent on the DoD and is written as

$$r_b = f\left(DoD\right)$$

Finally, the DoD is calculated from the cumulative charge as

5

$$DoD = \int I_b \frac{\left(\int I_b\right)^{-p_v}}{p_u} \in [0,1]$$

Where p_u and p_v parameterize the Peukert curve for the battery. This formulation is an oversimplification of the actual operation of the battery. It does not attempt to model any of the electrochemical processes that occur within. Characteristics of the battery may vary according to the severity and number of discharges. Moreover, batteries have the shortest life cycle of any electrical component in the powertrain. It is assumed that eternally fresh batteries are used in this vehicle.

The simple battery model can provide accurate gross performance predictions, and may be fruitfully used to compare competing battery management strategies. It is not useful for predicting battery transients or durability.

Inverter

The inverter is responsible for converting the battery's DC voltage to AC for the induction motor. It also reclaims energy created during regenerative braking to recharge the battery. The amplitude of the AC voltage is obviously limited by the battery voltage. The inverter model must enforce this limit, since the voltage output of the motor controller is not limited in any way.

A simplified model of the inverter, using only its fundamental frequency is implemented for real-time simulation. Since inverter outputs are usually filtered by the presence of an inductor, most of the harmonic content created by transistor switching is removed anyway. The simplified equations for six-step inverter operation are presented in [7]. The fundamental frequencies of the qd voltages during normal balanced operation are derived therein to be

$$v_{qs} = \frac{2}{\pi} v$$
$$v_{ds} = 0$$

(5)

Voltage and current controlled inverters driven by a vector control drive may depart from the normal output of (5), however, in response to a non-zero commanded d axis voltage. It is useful to define the 2-norms of the inverter voltage in the abc and qd reference frames for the purpose of limiting the inverter output. These norms are defined as

$$\left| v_{qd} \right|_2 = \sqrt{\frac{3}{2}\left(v_{qs}^2 + v_{ds}^2\right)}$$

(6)

and

$$\left| v_{abc} \right|_2 = \sqrt{\left(v_{as}^2 + v_{bs}^2 + v_{cs}^2\right)}$$

(7)

From (5) and (6), it is clear that the voltage norm of the inverter is limited to

$$\left| v_{max} \right|_2 = \frac{3}{\pi} v$$

The inverter implementation first converts the commanded voltages to the abc reference frame,

6

$$\vec{v}^{\,*}_{abc} = K^{-1} \vec{v}^{\,*}_{qd}$$

The three phase voltages are scaled if the norm of the command exceeds the maximum allowed by the battery.

$$\vec{v}_{abc} = \vec{v}^{\,*}_{abc} \min\left(1, \frac{|v_{max}|_2}{|v_{qd}|_2}\right)$$

Finally, the inverter output is obtained by transforming back to the qd reference frame

$$\vec{v}_{qd0} = K \vec{v}_{abc}$$

The transformation matrices are defined as

$$K = \frac{2}{3}\begin{bmatrix} \cos(\theta_e) & \cos\left(\theta_e - \frac{2\pi}{3}\right) & \cos\left(\theta_e + \frac{2\pi}{3}\right) \\ \sin(\theta_e) & \sin\left(\theta_e - \frac{2\pi}{3}\right) & \sin\left(\theta_e + \frac{2\pi}{3}\right) \\ \frac{1}{2} & \frac{1}{2} & \frac{1}{2} \end{bmatrix}$$

and

$$K^{-1} = \begin{bmatrix} \cos(\theta_e) & \sin(\theta_e) & 1 \\ \cos\left(\theta_e - \frac{2\pi}{3}\right) & \sin\left(\theta_e - \frac{2\pi}{3}\right) & 1 \\ \cos\left(\theta_e + \frac{2\pi}{3}\right) & \sin\left(\theta_e + \frac{2\pi}{3}\right) & 1 \end{bmatrix}$$

For reasons not fully understood by the author, proper operation of the vector controller-inverter-motor requires the inverter scaling to be performed in the abc reference frame rather than the qd frame.

Energy Management System

Hybrid electric vehicle configurations create added flexibility as well as added design complexity for the designer due to the extra degree of freedom obtained by having two power sources. This extra degree of freedom is managed in the energy management system (EMS). The role of the EMS in the current configuration is to set the desired torque of the motor as a function of the current vehicle behavior.

There are two main modes of operation of the motor. One is motor operation in which the motor assists the engine to accelerate the vehicle. The other is generator operation in which the motor either assists the passive brakes to decelerate or reclaims energy while coasting. Generator operation reverses the direction of power flow and actually charges the battery, a process known as regenerative braking. Note that regenerative braking does not only occur during driver braking. It may also occur on downhill slopes and if the battery's DoD exceeds an acceptable level. Regeneration during driving is not typically felt by the

7

driver, even though it is applying a braking torque to the vehicle. Rather, it is unconsciously corrected for with a slightly greater throttle input and engine torque, as if the vehicle were climbing a gentle grade.

A simple algorithm was used to determine the desired action of the motor. Desired motoring torque was set to some constant times the rotor angular acceleration. The constant is a function of the front driveline gear ratios and the desired authority of the motor. This simple strategy works as long as the engine and passive brakes maintain significant authority over vehicle performance. Then there will be strong coupling between the engine and braking torque and motor speed. The nice feature of this strategy is that it accommodates regenerative braking as well as motoring, except for the case in which the DoD has exceeded its threshold, and regeneration is independently commanded. In this case, a constant regenerative torque command is lowpass filtered to obtain a smooth evolution in motor behavior.

MOTOR FIDELITY COMPARISON

Simulations of the split hybrid vehicle quickly revealed that the induction motor model could not run at the same slow frequency as the rest of the system (240Hz). One possible remedy was to implement a multi-rate integration scheme that would allow the motor to run at a rate faster than the system frequency. Such an approach has worked well in the past [10]. Before committing to that solution, a comparison was made between the full order motor model and the simplified model, both described above. It was thought that if the simplified model offered practically equivalent performance and eliminated the need for multi-rate integration, it would be used instead of the full order model.

Offline simulation results are presented that indicate the simplified model is indeed sufficient for use in the context of real-time hybrid electric vehicle simulation. The simplified model neglects the transients in the stator as well as the 0s and 0r variables. These assumptions are valid and accurate for analysis if the supply voltage is balanced and transients are not modeled elsewhere in the power system. Both of these assumptions are valid in the HEV simulation environment.

The UDDS federal driving cycle was used to test three model variations. Variation one used the full order induction motor model with a system step size of 3.1ms. Variation two used the full order motor model with a step size of 3.2 ms. These two step sizes were chosen because they mark the loss of numerical stability during the simulation. Variation three used the simplified motor model with a step size of 4ms, the normal step size used for simulation in the NADS. A simulation length of 240 seconds was used, since that is when variation one began to exhibit instability.

Figure 2 shows the vehicle velocity in miles per hour on the UDDS driving cycle. Figure 3 shows motor torque for the three model variations. The subplot on the right shows a close-up of the torque plots. The close-up clearly shows the unstable behavior of variation one. The other two curves are grossly similar but there is an apparent difference in fine scale content. The only way to determine if the fine scale differences in the torque are detectable by the driver during a simulation is to look at the signals that are fed to the motion system. These signals are head point specific forces and head point angular velocities.

Figures 4 and 5 respectively show these signals. Once again, the subplots on the right show close-ups at the end of the simulation. The variation one instability is obvious. Specific forces from variations two and three are quite similar in amplitude and frequency, below the noise tolerance in the simulator (~10mG). Similarly, the angular velocities produced by variations two and three are very close in amplitude and frequency, at a level that would be considered small by a human driver (<3 deg/sec) [11].

It is concluded that the simplified model of the induction motor is more than adequate for all driver-in-the-loop (DITL) tests, and all but the highest fidelity of engineering applications. It should be noted that the full order model was less than a factor of two away from stable operation with the system step size of 4ms, well within the range of application of a multi-rate integration algorithm. A system upgrade would likely allow the system step size to be reduced anyway, a move that would be beneficial to other subsystems as well (e.g. tire models). At this time, little point is seen in accommodating the full order model given the low fidelity of the inverter and battery models.
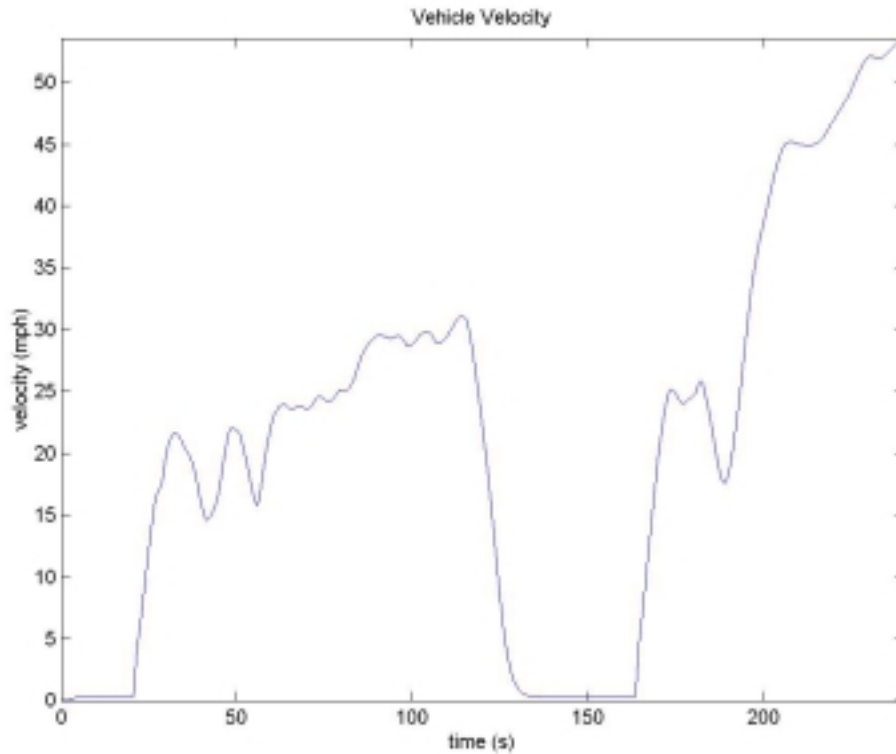
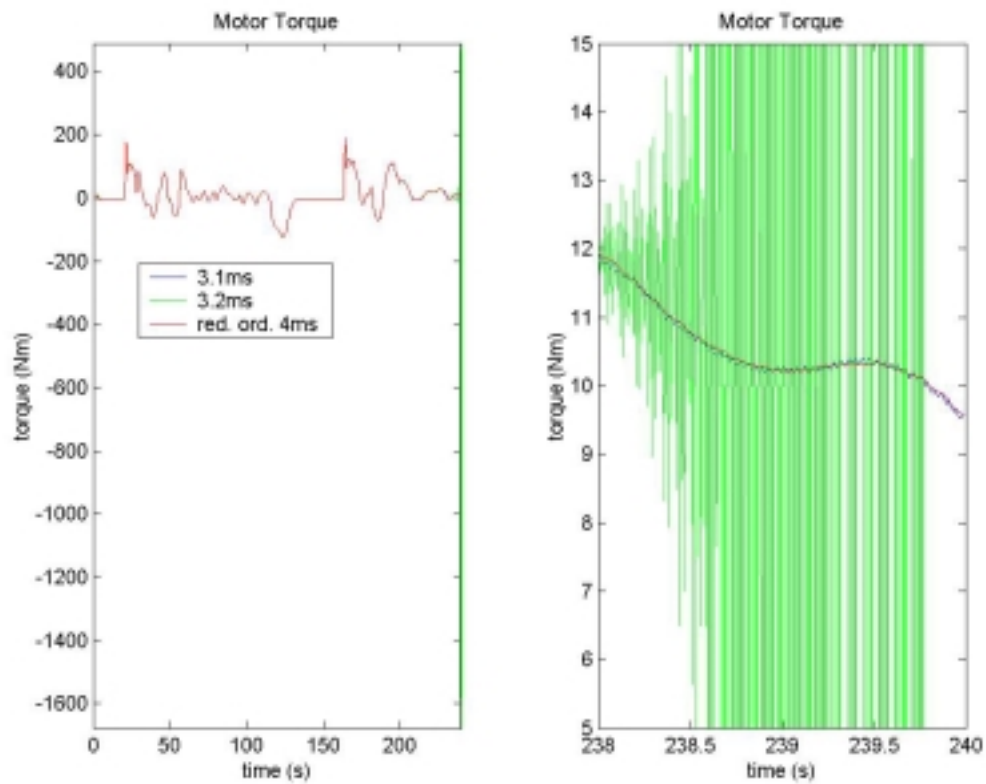**Figure 2. Vehicle Velocity during UDDS Driving Cycle**

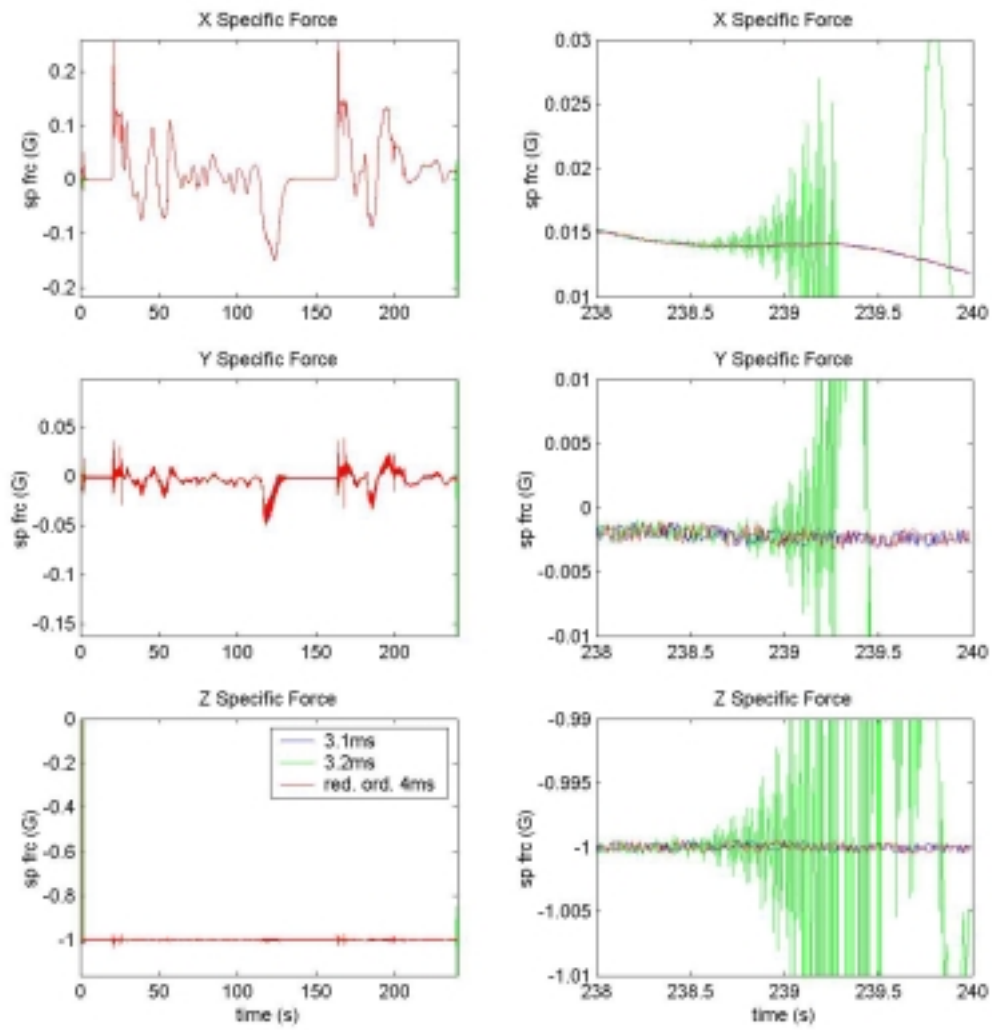**Figure 3. Induction Motor Torque during UDDS Driving Cycle**

9

Figure 4. Vehicle Translational Specific Forces during UDDS Driving Cycle
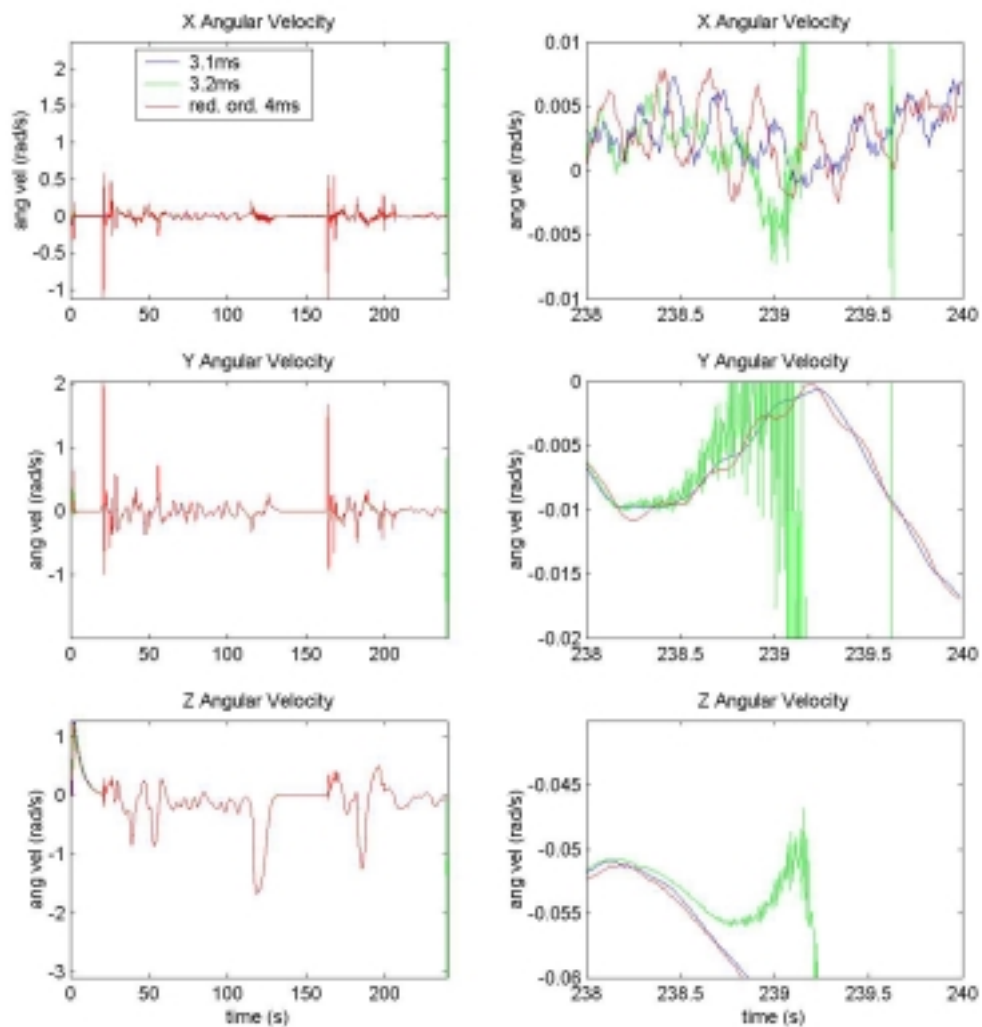
Figure 5. Vehicle Angular Velocities during UDDS Driving Cycle

MODEL DATA

Detailed model parameters for the conventional Jeep Cherokee can be found in [5,6]. Files that show how data has been modified for the hybrid Jeep design are shown here. Engine data is not listed here. It is merely the conventional Jeep engine torque data scaled to 70% of it original value.

11

Jeep_ttr_drive_line.inp

V1.08		
7		HYBRID 4 WHEEL DRIVE
0		RETARDER FLAG
0		TRACTION CONTROL FLAG
0.950000	0.950000	TRANSFER CASE EFFICIENCIES (low,high)
2.720000	1.000000	TRANSFER CASE GEAR RATIOS (low,high)
0.980000		FRONT DIFFERENTIAL EFFICIENCY
0.550000		FRONT DIFFERENTIAL SPEED RATIO
2.000000		FRONT TORSEN NULL BIAS RATIO RANGE
0.100000		FRONT TORSEN CONVERSION BIAS RATIO RANGE
2.000000		FRONT MAX TORQUE BIAS RATIO
0.980000		REAR DIFFERENTIAL EFFICIENCY
1.000000		REAR DIFFERENTIAL SPEED RATIO
2.000000		REAR TORSEN NULL BIAS RATIO RANGE
0.100000		REAR TORSEN CONVERSION BIAS RATIO RANGE
2.000000		REAR MAX TORQUE BIAS RATIO
0.980000	0.980000	FRONT FINAL DRIVE EFFICIENCIES (right,left)
3.550000	3.550000	FRONT FINAL DRIVE SPEED RATIOS (right,left)
0.980000	0.980000	REAR FINAL DRIVE EFFICIENCIES (right,left)
3.550000	3.550000	REAR FINAL DRIVE SPEED RATIOS (right,left)
0		Cruise control on [0: cruise control off]
1.000037		Accelerate parameter
3.0		Integrator controller gain
0.8		Proportional controller gain
10.0		Brake threshold to decativate cruise (N)
0.05		Throttle threshold to bypass cruise (%)
11.2		Cruise control cut off speed (m/sec)
0.5		Maximum throttle allowed (%)

battparams_ttr.inp

'Vb',   120.D0
'Vgen',   120.D0
'Vmot',   120.D0
'Vaux',   24.D0
'DoD_ini',0.2D0
'Pu',   277.D0
'Pv',   -0.11195
note: This file contains voltages for generator and auxiliary systems that are not used in the current configuration.

Imotor.100HP.L0228A

'p',   4.D0
'Wb',   377.d0
'Rs',   0.0174d0
'Rr',   0.0147d0
'Lls',   0.000134d0
'Llr',   0.00016d0
'Lms',   0.00464d0
'MFLAG',0
'EffMap',0
note: The MFLAG setting determines the use of the full order or simplified model. The EffMap flag indicates the absence or presence of efficiency map data.

CONCLUSIONS

A split configuration hybrid powertrain has been implemented in NADSdyna and connected to the Jeep Cherokee model. Offline tests indicate stable operation at the nominal dynamics step size. The split hybrid powertrain may be easily connected to other vehicle models. Moreover, previously developed series configuration hybrid powertrain may be easily substituted for the split configuration, although equivalent numerical stability properties cannot be guaranteed for all configurations.

The model described is appropriate for most vehicle simulations. A loss of accuracy may occur if: the three phase voltages are not balanced, transients are modeled in one part of the system but not another, or detailed battery performance is analyzed and compared to charging cycle measurements.

Future work will include additional electromechanical and electrochemical components. Additionally, the existing hybrid configurations will be combined into a common, general implementation.

ACKNOWLEDGEMENTS

REFERENCES

1. Durango to Get Patented Through-the-Road Hybrid Powertrain, http://www.daimlerchrysler.com/index_e.htm. Accessed July 22, 2001.

2. Garrott, W.R., et al., Methodology for Validating the National Advanced Driving Simulator's Vehicle Dynamics (NADSdyna), *SAE Paper 970563*, February 1997.

3. Salaani, M.K., Heydinger, G.J., and Guenther, D.A., Validation Results from Using NADSdyna Vehicle Dynamics Simulation, *SAE Paper 970565*, February 1997.

4. *NADS Vehicle Dynamics Simulation*, Release 4.0, Center for Computer-Aided Design, National Advanced Driving Simulator, The University of Iowa, Iowa City, IA, 1995.

5. Salaani, M.K., Guenther, D.A., and Heydinger, G.J., Vehicle dynamics Modeling for the National Advanced Driving Simulator of a 1997 Jeep Cherokee, *SAE International Congress & Exposition*, March 1999, Detroit, MI, pp. 47-63.

6. Salaani, M.K. and Heydinger, G.J., Model Validation of the 1997 Jeep Cherokee for the National Advanced Driving Simulator, *SAE 2000 World Congress*, Detroit, MI, March 2000, pp 1-7.

7. Krause, P.C., *Analysis of Electric Machinery*, McGraw-Hill, 1986.

8. Bose, B.K., *Power Electronics and AC Drives*, Prentice-Hall, New Jersey, 1986.

9. W.W. Marr, W.J. Walsh, and P.C. Symons, Modeling Battery Performance in Electric Vehicle Applications, *Energy Conversion Management*, Vol. 33, No. 9, 1992, pp. 843-847.

10. D. Solis and C.W. Schwarz, Multirate Integration in Hybrid Electric Vehicle Virtual Proving Grounds, *Proceedings of DETC'98 Design Automation Conference*, Atlanta, 1998.

11. Garrott, W.R., Simulator Motion Base Sizing Using Simulation, *SAE International Congress & Exposition*, March 1994, Detroit, MI, pp. 99-131.